Polymer Chemistry

Microfluidic-Supported Emulsion Polymerization: Molecular Weight and Concentration of Surface-Capping Agents Impacts Formation of Anisotropic Polyvinylmethacrylate Particles

Journal:	*Polymer Chemistry*
Manuscript ID	PY-ART-04-2025-000334
Article Type:	Paper
Date Submitted by the Author:	03-Apr-2025

Complete List of Authors:	Eisele, Dorthe; CUNY City College, Chemistry Visaveliya, Nikunjkumar; ChEmpower Corporation, ; Clarkson University, Kelestemur, Seda; The City College of New York, Chemistry and Biochemistry Khatoon, Firdaus; City College of the City University of New York, Xu, Jin; City College of the City University of New York Leo, Kelvin; City College of the City University of New York McCoy, Karisma; CUNY City College, Chemistry St. Peter, Lauren; City College of the City University of New York, Chan, Christopher; City College of the City University of New York Mikhailova, Tatiana; City College of the City University of New York, Bexheti, Visar; City College of the City University of New York, Shentolli, Geri; City College of the City University of New York, Biology Alagaratnam, Anushan; City College of the City University of New York Ahmed, Saad; City College of the City University of New York, Chem Maity, Piyali; City University of New York, Physics

ARTICLE

Microfluidic-Supported Emulsion Polymerization: Molecular Weight and Concentration of Surface-Capping Agents Impacts Formation of Anisotropic Polyvinylmethacrylate Particles.

Received 00th January 20xx,
Accepted 00th January 20xx

DOI: 10.1039/x0xx00000x

[#]Nikunjkumar R. Visaveliya[a], [#]Seda Kelestemur[a,b], Firdaus Khatoon[a], Jin Xu[a], Kelvin Leo[a], Karisma McCoy[a], Lauren St. Peter[a], Christopher Chan[a], Tatiana Mikhailova[a], Visar Bexheti[a], Geri Shentolli[a], Anushan Alagaratnam[a], Saad Ahmed[a], Piyali Maity[a], and Dorthe M. Eisele[a,c]*

Surface-capping agents—for example, amphiphilic surfactant molecules, water-soluble polymers, or polyelectrolytes—play a critical role during polymerization reactions for both formation and stability of colloidal polymer particles. Here, we investigated the effect of molecular weight and concentration of polymeric surface-capping agents on the assembling of polyvinyl methacrylate (PVMA) colloidal nanoparticles (NPs) via microfluidic-supported emulsion polymerization. Specifically, the impact of molecular weight and concentration of polyvinylpyrrolidone (PVP, molecular weights of 10,000, 40,000, 360,000, and 1,300,000 MW, concentrations of 0.05, 0.5, 1, 2.5, 5, and 10 mM, repeating unit concentration) and poly(sodium styrene sulfonate) (PSSS, molecular weights of 70,000 and 200,000 MW, concentrations of 0.1, 1, 2.5, 5, 10, and 20 mM, repeating unit concentration) on formation of PVMA NPs were investigated. Dependent on molecular weight and concentration of surface-capping agents, we obtained finely textured assembled, spherical, flower-shaped, fluffy, and elongated spherical PVMA NPs at sizes ranging from 70 to 500 nm. With our microfluidic-supported synthesis for PVMA NPs, we contributed to a basic understanding of how molecular weight and concentration of surface-capping agents impact the formation of polymer NPs.

INTRODUCTION

Colloidal polymer particles[1-7] are widely used in several applications such as; targeted drug delivery[8-10], tissue engineering[11], surface coating[12], and medical imaging [13, 14]. The interior and surface properties of the colloidal polymer particles play a crucial role during interaction with active surfaces of biological and non-biological materials.[15-23] In particular, the surface properties of colloidal polymer particles can be controlled post-synthetically *via* various techniques such as soft lithographic techniques or solvent evaporation processes.[24-27] However, the time-consuming post-synthetic treatments do not meet the requirements to control the size and shape of polymeric particles. Therefore, easy and rapid *in-situ* routes for controlling the structural surface properties of polymeric colloids are in high demand.

Emulsion polymerization is a versatile method to obtain colloidal particles with tunable sizes.[28-31] Molecular surfactants stabilize the surface of nanoparticles and simultaneously control the growth of particles in solution during polymerization.[32-34] Molecular surfactants, such as anionic sodium dodecyl sulfate (SDS) and cationic cetyltrimethylammonium bromide (CTAB), can form spherical micellar structures above their critical micelle concentration (CMC).[35] Surface-capping agents can also protect colloidal particles against uncontrolled aggregation.[33, 34] On the other hand, a polymeric surface-capping agent can act as a dynamic surface-controlling agent to initiate the assembling process of particles.[32, 36] Under controlled conditions, colloidal particles can create diverse structures from the nano- to sub-micron length scale that find use in a myriad of rheological and interfacial applications.[37-41] When soft polymer nanoparticles assemble during polymerization in a controlled manner, a wide range of anisotropic shapes can be generated.[42, 43] Compared to their spherical counterparts, anisotropic polymer nanoparticles are of particular importance due to their higher surface area (at the same length scale), making them suitable candidates for various medical applications.[44, 45]

[a] *Department of Chemistry and Biochemistry, The City College of The City University of New York, USA*
[b] *Biotechnology Department, Institute of Health Sciences, University of Health Sciences, Istanbul, Turkey*
[c] *Ph.D. Program in Chemistry, Graduate Center of The City University of New York, USA*

[#]The authors contributed equally

* Corresponding author: eisele@eiselegroup.com

The importance of molecular weight and concentration of surface-capping agents on particle shape and size was demonstrated in earlier studies[46-48]. Previously, the role of polymeric surface-capping agents in the generation of shape-tunable polymethylmethacrylate (PMMA) nanoparticles has been investigated in detail.[30, 42, 43] In addition, recently, the impact of five different types of surface-capping agents on the formation of colloidal polyvinylmethacrylate (PVMA) particles—employing the monomer unit with dual polymerization active sites—have been investigated.[49] In our previous work,[49] it was found that different types of surface-controlling agents have different roles in the formation of PVMA colloidal particles. Specifically, we showed that both the monomer type and interfacial agent has a role in controlling the anisotropic assembly pattern of colloidal PVMA NPs.[49] VMA is a non-viscous monomer suitable for several polymerization methods, for example, nitroxide-mediated polymerization. Nitroxide-mediated polymerization, a controlled radical polymerization, is generally used for styrene and acrylate-based monomers without any bulky group (including methyl) attached to their double bonds.[50, 51] In addition, VMA monomers and their derivatives also impact the reversible-addition–fragmentation chain-transfer (RAFT) polymerization.[52, 53]

In this work, we studied the impact of molecular weight and concentration of mainly two different types of polymeric surface-capping agents; (polymer polyvinylpyrrolidone (PVP) and polyelectrolyte poly(styrene sulfonate sodium salt) (PSSS)) on growth and *in-situ* assembly of PVMA colloidal particles via microfluidic-supported polymerization. We used non-ionic PVP at four different molecular weights (10,000, 40,000, 360,000, and 1,300,000 MW, concentrations of 0.05, 0.5, 1, 2.5, 5, and 10 mM, repeating unit concentration) and an anionic PSSS at two different molecular weights (70,000 and 200,000 MW, concentrations of 0.1, 1, 2.5, 5, 10, and 20 mM, repeating unit concentration) in the aqueous phase. We demonstrated that the assembling processes of colloidal PVMA particles can be controlled based on tunable molecular weights and concentrations of the surface-capping agents. The finely textured assembled, spherical, flower-shaped, fluffy, and elongated sphere PVMA NPs were obtained using PVP and PSSS. Utilization of a microfluidic platform[54-57] is a very efficient approach for providing uniform reaction mixing conditions. In our study, we used a cross-flow-based microfluidic reactor[35] for the emulsification of two immiscible liquid phases. The polymerization of the emulsified solution was performed externally as shown in **Figure 1** (semi-microfluidic process).

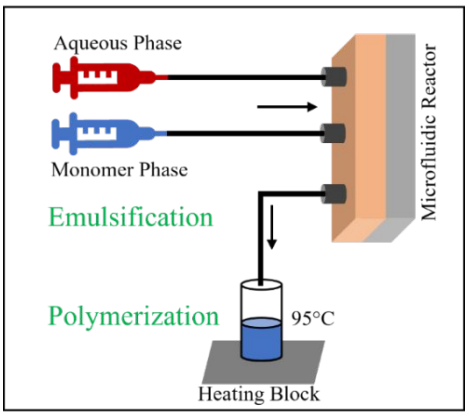

Figure 1: Experimental Setup. The Schematic illustrates the microfluidic-supported (semi-microfluidic) setup for the polymerization process in which emulsification of both immiscible liquid phases takes place in a microfluidic reactor and completion of the polymerization takes place at the heating block.

RESULTS AND DISCUSSION

The impact of PVA and PSSS at different molecular weights on the formation of PVMA colloidal particles was identified in the *in-situ* assembling of colloids in the aqueous phase. All molecular weights of the polymeric surface-controlling agents (PVP and PSSS) are considered in the gram per mole, and their concentration has been calculated based on their repeating unit concentration. Thermal polymerization was conducted by using a thermal initiator, azobisisobutyronitrile (AIBN) which was dissolved in the monomer phase including vinyl methacrylate (VMA) and ethylene glycol dimethacrylate (EGDMA) (**Figure 2**).

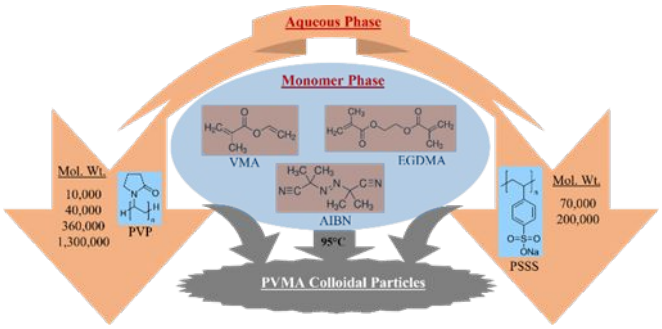

Figure 2: Schematic illustrates an overview of polymerization for the synthesis of PVMA NPs. The aqueous phase is made up of polymeric surface-capping agents of variable molecular weights and the monomer phase is a mixture of monomer, cross-linker, and thermal initiator. Polymerization was conducted at 95°C for the formation of PVMA colloidal particles.

1. Colloidal PVMA Particles: *Impact of tunable molecular weight and concentrations of PVP*

Here, the impact of non-ionic PVP with various molecular weights and concentrations on the formation of PVMA NPs was investigated. In general, during the emulsion polymerization, the interaction between the monomer droplets and PVP results in the formation of PVMA NPs. Initially, an emulsion of the VMA-contained monomer phase and PVP-contained aqueous phase is

generated in the microfluidic reactor, as shown in **Figure 1**. When the nucleation stage of the polymerization begins, the formation of small-sized nanoparticles (early growth state) is followed by continuous growth.[58] PVP, as a surface-capping agent, gets attached to the surface of growing colloidal NPs and controls the growth dynamics of the NPs. When water-soluble polymers are used, such as PVP, the control of surface properties of the growing NPs is driven by steric stabilization.[29]

The aggregation mechanism for the growth of PVMA NPs is comparable with the mechanism of PMMA NPs, as described previously.[30] In contrast to PMMA NPs synthesis, however, we obtained morphologically different PVMA NPs at various concentrations of PVP of tunable molecular weights. PVP controls the solvation and mobility of the growing PVMA NPs during the polymerization reaction. When particles are small (early growth stage), their solvation and mobility in an aqueous solution are high but when the particles' size is at the threshold level, particles assemble (aggregate) to reduce their surface energy[59]. Depending on the concentration and molecular weight of PVP, we obtained finely textured assembled, flower-shaped, and spherical PVMA NPs. Flower-shaped PVMA particles were obtained as a result of multi-step assembling processes at certain concentrations[30].

1.1. Utilizing PVP-10,000 (molecular weight) in aqueous phase

PVP-10,000 (concentrations at 0.5, 1, 5, and 10 mM, repeating unit concentration) were used to obtain PVMA NPs. 180 nm diameter finely textured surface PVMA NPs formed using 10 mM PVMA as depicted in **Figure 3A**. With the decrease of the PVP concentration down to 5 mM in the aqueous phase, no significant change in the obtained NPs was observed compared to using 10 mM PVP. In the case of using 5 mM PVP, the finely textured surface PVMA colloidal particles were obtained with a slightly smaller size in diameter of about 140 nm as shown in **Figure 3B**. Furthermore, the assembling pattern formed flower-shaped PVMA colloidal particles when PVP concentration was decreased to 1 mM repeating unit concentration (**Figure 3C**). According to our final products, we can conclude that the enhanced texture of the surface of PVMA colloidal particles formed due to the increased polymerization rate at lower PVP concentration. The number of formed PVMA particles is less at low PVP concentration and the polymerization rate is faster because the surface is slightly covered with a surface-capping agent (PVP). When polymerization is faster, the particles grow quickly before they achieve the aggregation stage and the aggregation is observed during the later phases of polymerization[60]. Indeed, larger PVMA aggregates and flower-shaped PVMA NPs were obtained at 1 mM concentration. With the further decrease of PVP concentration to 0.5 mM, spherical-shaped particles were obtained (**Figure 3D**). The final size of the spherical PVMA particles is smaller (less than 150 nm, **Figure 3D**) compared to the flower-shaped particles (**Figure 3C**). According to our final products, it can be assumed that the particles with textured surfaces as shown in **Figure 3A-C** are likely the result of aggregation of smaller-sized spherical NPs whereas the particles with smooth surfaces as shown in **Figure 3D** are individual particles formed without aggregation. The measured zeta potential of the PVP-covered PVMA colloidal particles is around -17 mM at all concentrations as shown in **Figure 3E**. The negative value of the zeta potential of PVMA colloidal particles may be a result of the enolization of the PVP in the aqueous phase as well as the radicals generated by the initiator AIBN[61, 62].

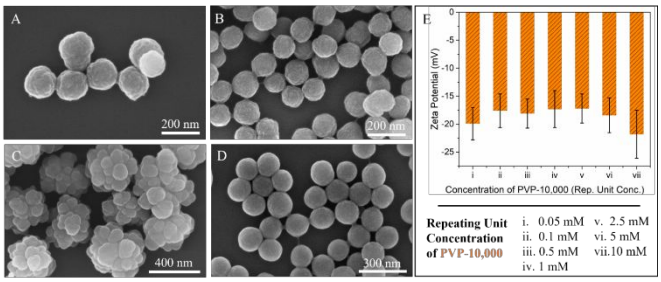

Figure 3: PVMA NPs upon using PVP-10,000 molecular weight in the aqueous phase. SEM images of the PVMA particles during the application of PVP-10,000 of various concentration in aqueous phase as a surface-capping agent: (A) 10 mM (repeating unit concentration), (B) 5 mM (repeating unit concentration), (C) 1 mM (repeating unit concentration), and (D) 0.5 mM (repeating unit concentration). (E) Zeta potential measurements of PVMA NPs formed using PVP-10,000 in the aqueous phase at various concentrations.

1.2 Utilizing PVP-40,000 (molecular weight) in aqueous phase

Large clustered and randomly aggregated PVMA NPs were obtained by using a 10 mM repeating unit concentration of PVP-40,000 as shown in **Figure 4A**. The observed surface texture of PVMA NPs that were obtained via using PVP at the same concentrations of 10,000 and 40,000 molecular weights are very different, as shown in **Figures 3A and 4A**, respectively. Also, the flower-shaped PMMA NPs with enhanced surface textures were obtained using different molecular weights of PVP than previously used for PVMA NPs [30]. This finding suggests that alongside the molecular weight and concentration of PVP, the type of monomer also has a significant impact on controlling the NP's surface characteristics.

When PVP-40,000 at 1 mM repeating unit concentration was used in the aqueous phase during polymerization, a progressive assembling pattern in the PVMA colloidal particles was observed as shown in **Figure 4B**. According to the aggregation behaviour of nanoparticles[59]; it is reasonable to assume that when the surface-capping agent concentration decreases, the growing particles prefer to minimize their surface energy as the surface is not densely covered with PVP. At 1 mM critical concentration, flower-shaped aggregates, and non-aggregated, rather 'fluffy' remaining products were observed (**Figure 4B**). With the further decrease of PVP-40,000 concentration in the aqueous phase (that is, 0.5 mM), almost all PVMA NPs formed in flower-shaped as shown in **Figure 4C**. Despite the long PVP chain, hydrophobic PVMA particles aggregated and formed textured surfaces due to the low concentration. Spherical type PVMA particles were obtained using PVP-40,000 at a concentration of 0.05 mM as shown in **Figure 4D**. The zeta potential of the PVMA NPs in the aqueous phase is shown in **Figure 4E**.

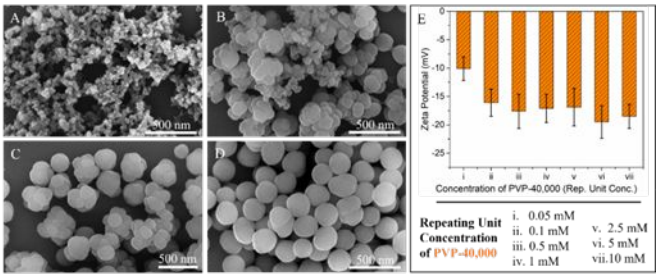

Figure 4: PVMA NPs during the applications of PVP-40,000 molecular weight in the aqueous phase. SEM images of PVMA NPs during application of PVP-40,000 of various concentration in aqueous phase as a surface-capping agent: (A) 10 mM (repeating unit concentration), (B) 1 mM (repeating unit concentration), (C) 0.5 mM (repeating unit concentration), and (D) 0.05 mM (repeating unit concentration). (E) Zeta potential measurements of the PVMA NPs formed using PVP-40,000 in the aqueous phase at various concentrations.

1.3 Utilizing PVP-360,000 (molecular weight) in aqueous phase

Finely textured assembled particles were obtained using 10 mM PVP-360,000 as shown in **Figure 5A**. When the concentration of PVP-360,000 decreased to 5 mM repeating unit concentration, rather 'fluffy' NPs were observed (**Figure 5B**). With the further decrease of the PVP-360,000 concentration (2.5 mM), non-assembled 'fluffy' NPs were observed (**Figure 5C**) similar to the NPs obtained using 10 mM PVP-40,000 in **Figure 4A**. No significant difference in the impact of 2.5 mM PVP-360,000 and 10 mM PVP-40,000 on NP's shape was observed (**Figure 4A and Figure 5C**). Spherical and 'fluffy' NPs were also obtained using 1 mM PVP-360,000 (**Figure 5D)**. Flower-shaped and spherical particles were obtained using 0.5 mM and 0.05 mM PVP-360,000 as shown in **Figure 5E** and **Figure 5F**, respectively. The zeta potentials of the obtained PVMA colloidal particles are shown in **Figure 5G**. The minor fluctuation observed in zeta potential values may be caused by the assembling patterns of the particles.

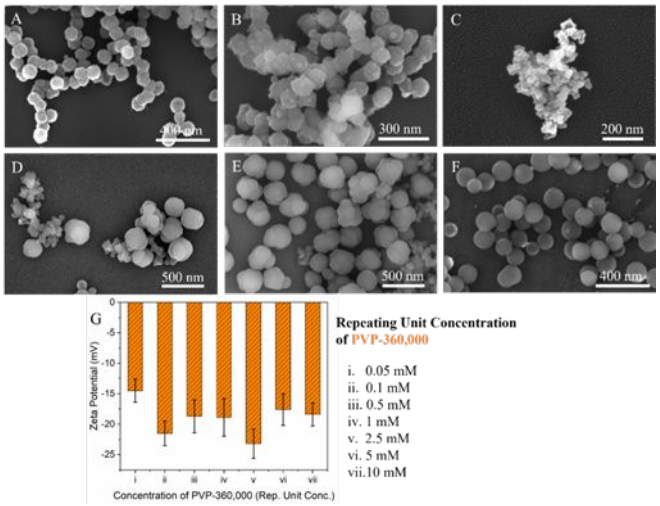

Figure 5. PVMA NPs during the applications of PVP-360,000 molecular weight in the aqueous phase. SEM images of the PVMA NPs during the application of PVP-360,000 of various concentration in aqueous phase as a surface-capping agent: (A) 10 mM (repeating unit concentration), (B) 5 mM (repeating unit concentration), (C) 2.5 mM (repeating unit concentration), and (D) 1 mM (repeating unit concentration), (E) 0.5 mM (repeating unit concentration), and (F) 0.05 mM (repeating unit concentration). (G) Zeta potential measurements of the PVMA NPs formed using PVP-360,000 in the aqueous phase at various concentrations.

1.4 Utilizing PVP-1,300,000 (molecular weight) in aqueous phase

The surface characteristics of PVMA NPs obtained using PVP-1,300,000 are very similar to the NPs obtained using PVP-360,000 (**Figure 5 and Figure 6**). Finely textured assembled particles were obtained using 10 mM PVP-1,300,000 (**Figure 6A**). In contrast, when the concentration decreased to 2.5 mM, dispersed 'fluffy' NPs were observed (**Figure 6B**). Flower-shaped NPs formed upon using 1 mM and 0.5 mM concentration of PVP-1,300,000 (**Figure 6C-D**). Moreover, larger textured assembly particles were formed at 0.1 mM concentration (**Figure 6E**). When high molecular weighed PVP was used at a lower concentration (0.05 mM), the polymerization created spherical type NPs with rather smooth surfaces as shown in **Figure 6F**. The zeta potential of the NPs was measured at about -17 mV (**Figure 6G**).

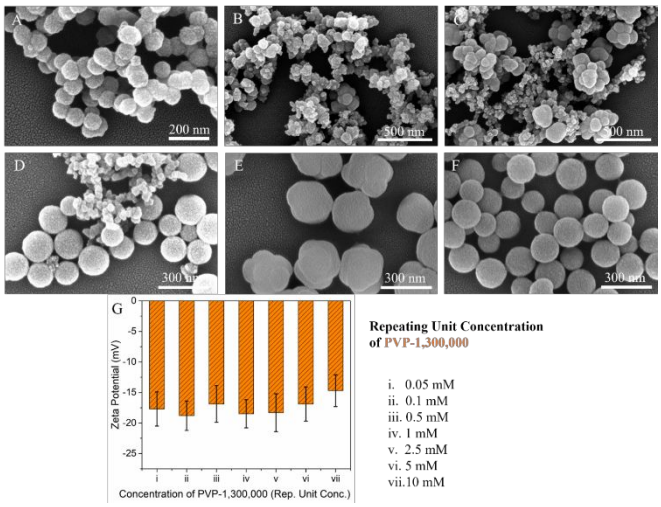

Figure 6: PVMA NPs during applications of PVP-1,300,000 molecular weight in the aqueous phase. SEM images of PVMA NPs during application of PVP-1,300,000 of various concentration in aqueous phase as a surface-capping agent: (A) 10 mM (repeating unit concentration), (B) 2.5 mM (repeating unit concentration), (C) 1 mM (repeating unit concentration), and (D) 0.5 mM (repeating unit concentration), (E) 0.1 mM (repeating unit concentration), and (F) 0.05 mM (repeating unit concentration). (G) Zeta potential measurements of the PVMA NPs formed using PVP-1,300,000 in the aqueous phase at various concentrations.

A schematic illustrating of the formation of PVMA colloidal particles using different molecular weights and concentrations of PVP is shown in **Figure 7**. Overall, based on the molecular weight and concentration, by utilization of PVP in the aqueous phase flower-shaped and spherical-shaped NPs were obtained.

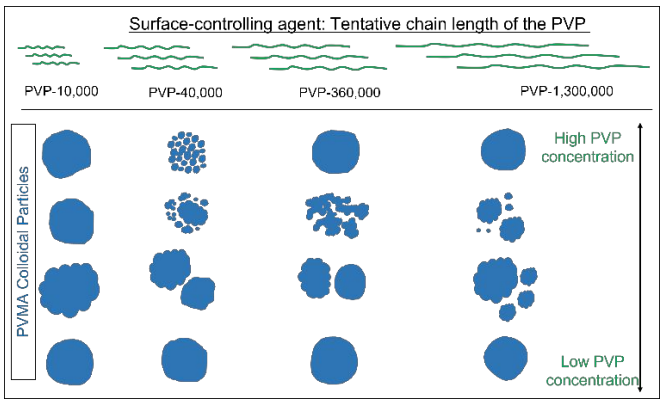

Figure 7: Schematic overview of the formation of PVMA NPs using different molecular weights and concentrations of PVP. The PVP chain length-based estimation of the molecular weights and the schematics of the PVMA NPs obtained at higher and lower concentrations by application of PVP of various molecular weights.

2. Colloidal PVMA Particles: *Impact of tunable molecular weight and concentrations of PSSS*

PSSS is an anionic polyelectrolyte and contains a large number of sulfonate ions. Two different molecular weights of PSSS (70,000 and 200,000) were used at six different concentrations (0.1mM to 20 mM). The linear assembly pattern of PVMA NPs is similar to the assembling pattern of PMMA NPs.[42, 43]

2.1 Utilizing PSSS-70,000 (molecular weight) in aqueous phase

Here, we used PSSS-70,000 in the aqueous phase during polymerization. When 20 mM PSSS-70,000 was used in the aqueous phase, elongated sphere PVMA colloidal particles were obtained (**Figure 8A**). On the other hand, elongated assembled PMMA NPs can also be obtained by using PSSS-70,000.[43] This comparison shows that not only the PSSS molecular weights but also the type of monomer are very effective on the final NP shape. When the concentration of PSSS-70,000 decreased from 20 mM to 10 mM, 2.5 mM, and 1 mM (repeating unit concentrations), spherical PVMA NPs were obtained in all cases as shown in **Figure 8B-D**. Zeta potential value is dependent on the charge and concentration of surface capping agents on the surface of polymeric nanoparticle. The zeta potential value of the PVMA NPs increased in the negative direction correlatedly with the increase of anionic PSSS concentration as shown in **Figure 8E**.

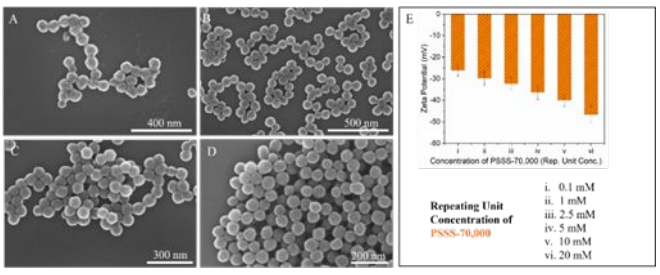

Figure 8. PVMA NPs were obtained during the applications of PSSS-70,000 molecular weight. SEM images of the PVMA NPs during various concentrations of anionic polyelectrolyte PSSS-70,000 in aqueous phase as a surface-capping agent: (A) 20 mM (repeating unit concentration), (B) 10 mM (repeating unit concentration), (C) 2.5 mM (repeating unit concentration), and (D) 0.1 mM (repeating unit concentration). (E) Zeta potential measurements of PVMA NPs formed using PSSS-70,000 in the aqueous phase at various concentrations.

2.2 Utilizing PSSS-200,000 (molecular weight) in aqueous phase

Linear direction assembled elongated sphere PVMA were obtained using 20 mM (repeating unit concentration) PSSS-200,000 as shown in **Figure 9A**. It is hypothesized that the PSSS chains breaking apart due to the assembling of hydrophobic entities in the aqueous solution resulted in linearly assembled PVMA nanoparticles[43]. The linear directed assembled PVMA NPs obtained using 5 mM, 1 mM, and 0.5 mM (repeating unit concentrations) PSSS-200,000 are shown in **Figures 9B, 9C, and 9D**, respectively. The zeta potentials of the NPs are strongly dependent on the concentration of PSSS. The zeta potential values of the NPs decreased with increasing PSSS concentration in the aqueous phase as shown in **Figure 9E.**

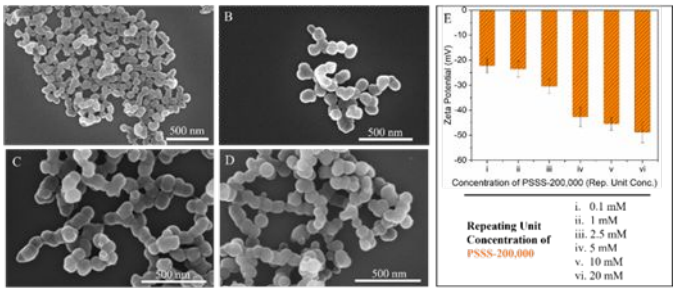

Figure 9: PVMA NPs were obtained during applications of PSSS-200,000 molecular weight in the aqueous phase. SEM images of the PVMA NPs during various concentrations of anionic polyelectrolyte PSSS-200,000 in aqueous phase as a surface-capping agent: (A) 20 mM (repeating unit concentration), (B) 5 mM (repeating unit concentration), (C) 1 mM (repeating unit concentration), and (D) 0.1 mM (repeating unit concentration). (E) Zeta potential measurements of the PVMA NPs formed using PSSS-200,000 in the aqueous phase at various concentrations.

CONCLUSIONS

In our work, the formation of in-situ assembled PVMA NPs is demonstrated by using surface-capping agents, PVP, and PSSS, of tunable molecular weights and concentrations via semi-microfluidic emulsion polymerization. The molecular weight and concentration of surface-capping agents influenced the assembling process, resulting in the formation of anisotropic PVMA NPs with various shapes. Specifically, fine textured NPs were obtained at high PVP concentrations (5 mM to 10 mM, molecular weight dependent), while flower-shaped NPs were obtained at lower concentrations (0.5 mM to 1 mM, molecular weight dependent). Reducing the concentration of PVP (0.05 mM to 0.5 mM, molecular weight dependent) resulted in the formation of spherical NPs at all molecular weights. Elongated sphere and spherical PVMA NPs were obtained using PSSS (70,000, molecular weight), while linear directed assembled elongated spherical NPs formed using PSSS (200,000, molecular weight), regardless of concentration. Controlling the self-assembly of soft polymeric materials is challenging in a single-step continuous polymerization. We developed a controllable microfluidic-supported method to tune the surface properties of the PVMA NPs. New synthesis strategies require to be explored in a wide range of various polymeric systems for generating a diverse structure of biocompatible and biodegradable

nanoparticles useful in a broad spectrum of biological applications.

Experimental Section

Materials and chemicals

Vinyl methacrylate (VMA) (Sigma-Aldrich, 98%), ethylene glycol dimethacrylate (EGDMA) (Sigma-Aldrich, 98%), azobisisobutyronitrile (AIBN) (Sigma-Aldrich, 98%), poly(styrene sulfonate sodium salt) (PSSS, 70,000 MW, 200,000 MW, Sigma-Aldrich), polyvinyl pyrrolidone (PVP, 10,000 Mw, 40,000 MW, 360, 000 MW, 1,300,000 MW, Sigma-Aldrich) used as received without further purification. Ultrapure water (Milli-Q) was used in all experiments.

Microfluidic-supported synthesis of PVMA NPs

In this study, a microfluidic reactor[35] was used for the formation of an emulsion of two immiscible liquid phases and conducting emulsion polymerization. The microreactor was fabricated *via* lithography technique[35]. The microfluidic-supported emulsification of two immiscible liquids and their polymerization on the heating block outside the microfluidic reactor is given in **Figure 1**. The emulsification of both immiscible phases takes place in the microreactor, but the polymerization is completed on the heating block.

The formation of PVMA nanoparticles was performed by emulsion polymerization. Two immiscible liquid phases were prepared separately for emulsification: an aqueous phase (continuous phase) and a monomer phase (dispersed phase). The aqueous phase is composed of surface-capping agents (PSSS or PVP) at different molecular weights and concentrations. The monomer phase is composed of a mixture of vinyl methacrylate (VMA, monomer), ethylene glycol dimethacrylate (EGDMA, cross-linker), and azobisisobutyronitrile (AIBN, thermal initiator). For preparing 1 mL of monomer phase solution, 4 µg AIBN and 10 µL EGDMA were dissolved in 990 µL of VMA. For the microfluidic system, pumps from New Era Pump System Inc. were used as shown in **Figure 1**. 1200 µL/min flow rate was used for the monomer phase and 80 µL/min flow rate was used for the aqueous phase. The emulsion was obtained by mixing two immiscible phases in a microfluidic platform and the polymerization took place in a small vial on the heating block at 95°C for 20 min (**Figure 1**). The PVMA NPs washed with ultrapure water by two-cycle of centrifugation (11,000 RPM, 12 minutes) using a Thermo Fisher Company centrifuge. The purified PVMA NPs were characterized by Scanning Electron Microscopy (SEM) and zeta sizer.

Characterization of PVMA NPs

Scanning electron microscopy (SEM) characterization

10 µL of PVMA nanoparticles were diluted with ultra-pure water to 100 µL (dilution) before SEM measurements. A silicon chip (made a small piece of 1 cm x1 cm from the silicon wafer by micro cutter) was used for preparing the samples for characterization. The sample on the silicon chip was covered with gold using Leica EM ACE600 Coater (thickness: 2.7 nm). FEI Helios Nanolab 660 FIB-SEM was used for the characterization of PVMA nanoparticles. Images were taken at 5 kV voltage and 25 pA current at multiple magnifications.

Zeta potential measurements

The Zeta potential of PVMA nanoparticles was measured by the Malvern Zetasizer instrument (Zetasizer Nano Series: Nano ZS). Initially, the centrifuged particles were re-dispersed in ultrapure water. 50 µL of nanoparticle dispersion diluted to 1 mL using ultra-pure water. Malvern: DTS1070 cells were used for zeta potential measurements.

Author Contributions

D.M.E. directed the project; N.R.V. designed experiments; F.K., J.X., K.L., K.M., and L.S.P. supported the experimental setup and synthesis of colloidal polymer nanoparticles; J.X., C.C., T.M., and V.B. supported in purification and characterization of polymer nanoparticles; F.K. and L.S.P. supported in SEM imaging; J.X., G.S., A.A., S.A., L.S.P., K.L., and F.K. supported in zeta potential measurements; P.M. and S.K. provided data interpretation and fruitful discussions during the preparation of the manuscript; D.M.E., S.K., N.R.V. co-wrote the manuscript with inputs from all co-authors.

Conflicts of interest

There are no conflicts to declare.

Acknowledgements

This material is based upon work partially supported by the National Science Foundation Faculty Early Career Development Program (NSF-CAREER 1752475) and the U.S. Department of Energy, Office of Science, Office of Basic Energy Sciences (DOE DE-SC0018142). Equipment support is partially provided by the National Science Foundation Major Research Instrumentation Program (NSF-MRI 1531859). Support partially provided by the National Science Foundation NSF-CREST Center for Interface Design and Engineered Assembly of Low Dimensional Systems (IDEALS), NSF grant number NSF-CREST HRD-1547830. This work was performed at the Center for Discovery and Innovation of The City College of New York and the Advanced Science Research Center Imaging Facility of The City University of New York. The authors thank PSC-CUNY Research Award Program for its support.

References

1. S. Haddadi, M. Skepö, P. Jannasch, S. Manner and J. Forsman, *Journal of Colloid and Interface Science*, 2021, **581**, 669-681.

2. M. J. Monteiro and M. F. Cunningham, *Biomacromolecules*, 2020, **21**, 4377-4378.

3. R. M. Fitch, *British Polymer Journal*, 1973, **5**, 467-483.

4. R. Deng, L. Zheng, X. Mao, B. Li and J. Zhu, *Small*, 2021, **17**, 2006132.

5. J. L. Ortega-Vinuesa, A. Martín-Rodríguez and R. Hidalgo-Álvarez, *Journal of Colloid and Interface Science*, 1996, **184**, 259-267.

6. F. Tiarks, K. Landfester and M. Antonietti, *Langmuir*, 2001, **17**, 908-918.

7. A. Musyanovych and K. Landfester, *Macromolecular Bioscience*, 2014, **14**, 458-477.

8. E. W. Durbin and G. A. Buxton, *Soft Matter*, 2010, **6**, 762-767.

9. K. Loomis, K. McNeeley and R. V. Bellamkonda, *Soft Matter*, 2011, **7**, 839-856.

10. M. Elsabahy and K. L. Wooley, *Chemical Society Reviews*, 2012, **41**, 2545-2561.

11. W. Li, L. Zhang, X. Ge, B. Xu, W. Zhang, L. Qu, C.-H. Choi, J. Xu, A. Zhang, H. Lee and D. A. Weitz, *Chemical Society Reviews*, 2018, **47**, 5646-5683.

12. S. Jiang, A. Van Dyk, A. Maurice, J. Bohling, D. Fasano and S. Brownell, *Chemical Society Reviews*, 2017, **46**, 3792-3807.

13. T. Repenko, A. Rix, S. Ludwanowski, D. Go, F. Kiessling, W. Lederle and A. J. C. Kuehne, *Nat Commun*, 2017, **8**, 470.

14. M. Elsabahy, G. S. Heo, S.-M. Lim, G. Sun and K. L. Wooley, *Chemical Reviews*, 2015, **115**, 10967-11011.

15. S. Liu, R. Deng, W. Li and J. Zhu, *Advanced Functional Materials*, 2012, **22**, 1692-1697.

16. M. P. Robin and R. K. O'Reilly, *Polymer International*, 2015, **64**, 174-182.

17. K. Kempe, R. A. Wylie, M. D. Dimitriou, H. Tran, R. Hoogenboom, U. S. Schubert, C. J. Hawker, L. M. Campos and L. A. Connal, *Journal of Polymer Science Part A: Polymer Chemistry*, 2016, **54**, 750-757.

18. M. Szczęch and K. Szczepanowicz, *Nanomaterials*, 2020, **10**, 496.

19. W. Wichaita, Y.-G. Kim, P. Tangboriboonrat and H. Thérien-Aubin, *Polymer Chemistry*, 2020, **11**, 2119-2128.

20. M. A. C. Stuart, W. T. S. Huck, J. Genzer, M. Muller, C. Ober, M. Stamm, G. B. Sukhorukov, I. Szleifer, V. V. Tsukruk, M. Urban, F. Winnik, S. Zauscher, I. Luzinov and S. Minko, *Nat Mater*, 2010, **9**, 101-113.

21. A. Lendlein and V. P. Shastri, *Advanced Materials*, 2010, **22**, 3344-3347.

22. S. Mura, J. Nicolas and P. Couvreur, *Nature Materials*, 2013, **12**, 991-1003.

23. X. Liu, Y. Yang and M. W. Urban, *Macromolecular Rapid Communications*, 2017, **38**, 1700030.

24. N. R. Visaveliya, C. W. Leishman, K. Ng, N. Yehya, N. Tobar, D. M. Eisele and J. M. Köhler, *Advanced Materials Interfaces*, 2017, **4**, 1700929.

25. M. Božič, T. Elschner, D. Tkaučič, M. Bračič, S. Hribernik, K. Stana Kleinschek and R. Kargl, *Cellulose*, 2018, **25**, 6901-6922.

26. T. Urbaniak and W. Musiał, *Nanomaterials*, 2019, **9**, 1240.

27. L. Yu, N. Zhang, N.-N. Zhang, Q. Gu, Y. Xue, Y.-X. Wang, C.-L. Han, K. Liu, Z.-Y. Sun, H.-J. Qian and Z.-Y. Lu, *The Journal of Physical Chemistry Letters*, 2021, **12**, 7100-7105.

28. C. S. Chern, *Progress in Polymer Science*, 2006, **31**, 443-486.

29. P. A. Lovell and F. J. Schork, *Biomacromolecules*, 2020, **21**, 4396-4441.

30. N. Visaveliya and J. M. Köhler, *Langmuir*, 2014, **30**, 12180-12189.

31. A. Gharieh, S. Khoee and A. R. Mahdavian, *Advances in Colloid and Interface Science*, 2019, **269**, 152-186.

32. H. Heinz, C. Pramanik, O. Heinz, Y. Ding, R. K. Mishra, D. Marchon, R. J. Flatt, I. Estrela-Lopis, J. Llop, S. Moya and R. F. Ziolo, *Surface Science Reports*, 2017, **72**, 1-58.

33. J. P. Rao and K. E. Geckeler, *Progress in Polymer Science*, 2011, **36**, 887-913.

34. T. Al Najjar, N. K. Allam and E. N. El Sawy, *Nanoscale Advances*, 2021, **3**, 5626-5635.

35. J. M. Koehler, F. Moeller, S. Schneider, P. M. Guenther, A. Albrecht and G. A. Gross, *Chemical Engineering Journal*, 2011, **167**, 688-693.

36. S. Javadian and J. Kakemam, *Journal of Molecular Liquids*, 2017, **242**, 115-128.

37. E. A. Appel, M. W. Tibbitt, M. J. Webber, B. A. Mattix, O. Veiseh and R. Langer, *Nature Communications*, 2015, **6**, 6295.

38. E. L. Correia, N. Brown and S. Razavi, *Nanomaterials*, 2021, **11**, 374.

39. N. J. Alvarez, S. L. Anna, T. Saigal, R. D. Tilton and L. M. Walker, *Langmuir*, 2012, **28**, 8052-8063.

40. M. Urban, B. Freisinger, O. Ghazy, R. Staff, K. Landfester, D. Crespy and A. Musyanovych, *Macromolecules*, 2014, **47**, 7194-7199.

41. H. Zou and S. Zhai, *Polymer Chemistry*, 2020, **11**, 3370-3392.

42. N. Visaveliya and J. M. Kohler, *Acs Appl Mater Inter*, 2014, **6**, 11254-11264.

43. N. Visaveliya and J. M. Kohler, *Macromolecular Chemistry and Physics*, 2015, **216**, 1212-1219.

44. J. A. Champion and S. Mitragotri, *Proceedings of the National Academy of Sciences of the United States of America*, 2006, **103**, 4930-4934.

45. O. C. Farokhzad and R. Langer, *Acs Nano*, 2009, **3**, 16-20.

46. H. Minami, K. Yoshida and M. Okubo, *Macromol Rapid Comm*, 2008, **29**, 567-572.

47. S. Shen, E. D. Sudol and M. S. Elaasser, *J Polym Sci Pol Chem*, 1993, **31**, 1393-1402.

48. T. H. Yang, Y. F. Shi, A. Janssen and Y. N. Xia, *Angew Chem Int Edit*, 2020, **59**, 15378-15401.

49. N. R. Visaveliya, S. Kelestemur, F. Khatoon, J. Xu, K. Leo, L. St. Peter, C. Chan, T. Mikhailova, V. Bexheti, A. Kapadia, P. Maity, W. P. Carbery, K. Ng and D. M. Eisele, *Polymer Chemistry*, 2022, **13**, 4625-4633.

50. J. Nicolas, Y. Guillaneuf, C. Lefay, D. Bertin, D. Gigmes and B. Charleux, *Progress in Polymer Science*, 2013, **38**, 63-235.

51. W. A. Braunecker and K. Matyjaszewski, *Progress in Polymer Science*, 2007, **32**, 93-146.

52. S. Perrier, *Macromolecules*, 2017, **50**, 7433-7447.

53. S. Harrisson, X. Liu, J.-N. Ollagnier, O. Coutelier, J.-D. Marty and M. Destarac, *Polymers*, 2014, **6**, 1437-1488.

54. R. Karnik, F. Gu, P. Basto, C. Cannizzaro, L. Dean, W. Kyei-Manu, R. Langer and O. C. Farokhzad, *Nano Letters*, 2008, **8**, 2906-2912.

55. C. N. Baroud, F. Gallaire and R. Dangla, *Lab on a Chip*, 2010, **10**, 2032-2045.

56. C. A. Serra and Z. Q. Chang, *Chemical Engineering & Technology*, 2008, **31**, 1099-1115.

57. J. M. Kohler, S. N. Li and A. Knauer, *Chemical Engineering & Technology*, 2013, **36**, 887-899.

58. Z. Hua, J. R. Jones, M. Thomas, M. C. Arno, A. Souslov, T. R. Wilks and R. K. O'Reilly, *Nat Commun*, 2019, **10**.

59. S. Shrestha, B. Wang and P. Dutta, *Adv Colloid Interfac*, 2020, **279**.

60. B. J. Liu, Y. J. Wang, M. Y. Zhang and H. X. Zhang, *Polymers-Basel*, 2016, **8**.

61. G. Oster and E. H. Immergut, *J Am Chem Soc*, 1954, **76**, 1393-1396.

62. M. Yamashina, Y. Sei, M. Akita and M. Yoshizawa, *Nat Commun*, 2014, **5**.

Data availability. All data used in this report has been included in the paper.